EXPERIMENTAL DETERMINATION OF HADRONIC CONSTITUENT SCATTERING

A proposal to measure the energy, angular, and charge dependence of massive di-hadron production over a large solid angle in intense proton and pion beams.

D. Levinthal, S. H. Pordes, P. A. Rapidis, and H. B. White
Fermi National Accelerator Laboratory

J. L. Pinfold
Carleton University

M. J. Oreglia
University of Chicago

H. R. Gustafson
University of Michigan

M. B. Crissler and J. T. Volk
Ohio State University

N. D. Giokaris
University of Rochester

R. L. Messner
Stanford Linear Accelerator Center

T. Cardello
Yale University

Scientific Spokesperson: D. Levinthal

Abstract

We propose to measure the wide angle production of massive di-hadrons with pion and proton beams using a high resolution, large aperture magnetic spectrometer. The di-hadron continuum provides the most direct method of measuring the energy, angular and flavor dependence of the quark-quark scattering cross section.

While it is generally agreed upon that hadronic matter is composed of quarks, the basic quark-quark scattering amplitudes are still unknown. We propose to measure the energy, angular and flavor dependence of the quark-quark scattering amplitudes using events selected by a 2-particle symmetric high P_T trigger. In addition we will measure the angular dependence of single charged particle inclusive cross sections in the presently unexplored region of $7\ GeV \leq P_T \leq 14\ GeV$.

Previous experiments have shown that when one triggers on a single high P_T particle, several properties of the event are apparent (see appendix A).

1. A jet like structure is observed recoiling from the trigger particle if its transverse momentum is sufficiently high ($P_T > 7$ GeV).[1]
2. The trigger particle is associated with accompanying hadrons in strong spatial correlation (jet).[1]
3. Perhaps most important, the fraction of the trigger side jet momentum (Z_{trig}) taken by the trigger particle ranges from 75% to 90%, increasing with $x_T = 2P_T/\sqrt{s}$.[2,6]

The existence of an isolated recoiling system makes it natural to conclude that high P_T hadron production is due to the wide angle scattering of hadronic constituents. Furthermore, when events are selected by requiring the presence of a single high P_T hadron (as opposed to "jet"

triggers), the trigger hadron momentum can be used as an accurate approximation of the scattered parton momentum due to the large value of Z_{trig}.

Attempts to exploit this feature of high p_T production by measuring only one of the parent partons have failed to fully measure the quark-quark scattering amplitudes. The uncertainty due to the Fermi motion and the tendency for the initial state to be moving in the trigger direction complicate the interpretation of single particle measurements.[3] A more serious failure is the absence of any information on the recoil system kinematics. Consequently, with a single particle trigger, only part of the functional dependence of the cross section is measured. These problems can be greatly reduced by taking symmetrically triggered events.[4]

Symmetric trigger

Events selected by requiring two roughly back to back high P_T particles eliminate many of the problems intrinsic to the single arm trigger. There is no bias favoring events with the initial state partons moving in one direction or the other. Of greater importance, all the kinematics of the scattered constituents are measured, not just the momentum transfer as in single particle measurements. To illustrate

this, consider two high P_T hadrons recoiling from each other at $X_F = 2(P_{z1}-P_{z2})/\sqrt{s}$ of approximately zero. In the limit that their transverse momenta balance, then the mass of the di-hadron system is an approximation of the C of M parton-parton scattering energy ($\sqrt{\hat{s}}$) and the angle of the di-hadron axis relative to the beam line is the parton-parton scattering angle. Thus, by studying the angular dependence of the di-hadron axis at $X_F \sim 0$ one can study the angular dependence of the parton-parton interaction.

The importance of doing the measurement at $X_F \sim 0$ is to insure that both target and beam quarks are in the valence region (i.e. $x > 0.3$). At $X_F > 0.2$ the target quark does not satisfy this condition except at <u>extremely</u> large $x_1x_2 = m^2/S$. The mass and $X(\sim m/\sqrt{s})$ dependence of the angular distribution can be separately studied by running at different beam energies and the degree to which the cross section can be factorized in these variables explicity measured. This aspect of the measurement is free of two serious difficulties involved in the one particle experiment. There, cross sections from two different energies must be used and a form assumed for the cross section (a scaling law $\frac{A}{p_T^n} F(x)$) in order to extract any useful information. In contrast, one angular distribution at fixed mass and fixed beam energy has a straight forward

interpretation as the angular dependence of the differential cross section $\frac{d^2\sigma}{dEd\cos\theta}$ for elastic quark-quark scattering at fixed energy. A parallel can be drawn between this measurement and the angular distributions for $e^+e^-\rightarrow\mu^+\mu^-$ (figure 2) where the functional dependence of the scattering cross section is studied and thereby the force law. The di-hadron experiment can be viewed as the same type of measurement but with a "wide band" intersecting quark beam.

The mass cross section (integrated over a fixed range of $\cos\theta$) at two (or more) energies can be fit to the form $\frac{A}{m^n}F(x)$, with the power n indicating the functional dependence of the scattering on the parton energy (the energy dependence of $d^2\sigma/dEd\cos\theta$). This corresponds to the method used in the inclusive one particle measurement where the same assumption of a scaling form for the cross section is made in the fit $\frac{A}{P_T^n}F(x)$. For such a measurement, calculations have indicated that the Fermi motion severely changes the power law ($\Delta n\sim 2$) for the one particle final state. For the symmetric trigger the Fermi motion has virtually no effect.

If one further includes the charge correlation observed in $\bar{\nu}$ interactions,[5] the di-hadron measurement takes an even greater significance. Then the angle, energy, and flavor dependence of the scattering cross section can be measured.

Given the large value of Z for high p_T particles it is natural to assume that positively charged hadrons at high p_T come from positively charged quarks $(u,\bar{d})$ and negatively charged hadrons come from negatively charged quarks $(\bar{u},d)$. If the measurement is done at a mass such that $m/\sqrt{s} \sim 0.3$ or greater, then only valence partons need be considered. In this case, the following initial and final states could be interpreted in the quark model as follows:

$pN \rightarrow h^+h^+$ due to uu scattering

$\rightarrow h^+h^-$ due to ud scattering

$\rightarrow h^-h^-$ due to $\bar{d}d$ scattering.

$\pi^+N \rightarrow h^+h^+$ due to $uu+\bar{d}u$ scattering

$\rightarrow h^+h^-$ due to $ud+\bar{d}d$ scattering

$\pi^-N \rightarrow h^+h^-$ due to $\bar{u}u+du$ scattering

$\rightarrow h^-h^-$ due to $\bar{u}d+dd$ scattering.

Final states of the form

$$\pi^-N \rightarrow h^+h^+ \text{ or } \pi^+N \rightarrow h^-h^-$$

do not occur in this simple model. However their rates relative to those of the valence diagrams will indicate the rate of wrong sign fragmentation and the relative abundance of sea quark and gluon diagrams. In the case of the πN collisions for the h^+h^- final state not only the magnitude of $\cos\theta$ is measured but its sign as well.

Requirements of the measurement.

In view of the physics potential of this measurement a dedicated experiment is appropriate. The ISR data on massive di-hadrons[6] consist of $\pi^o\pi^o$, $(+\pi^o\eta^o + \pi^o\gamma$ etc) data collected with lead glass arrays. This type of measurement (i.e. calorimetric) is sensitive to absolute calibration uncertainty and multi particle overlaps, both of which could be angle dependent. Small calibration errors ($\sim$3%) which vary systematically over the face of the calorimeter distort the angular distribution significantly (by $\sim$ 20%). The overlap problem is severe simply because of the poor spatial resolution of calorimetric devices. It is therefore essential to do this measurement with a high resolution tracking system.

The ISR data indicate a strong dependence of the cross section at fixed mass with $|\cos\theta|$. The ratio of the cross section between $\cos\theta$ of 0 and 0.5 is a factor of 4.

However, between 0 and 0.25 the ratio is only a factor of 1.4. Therefore to measure this cross section well, a large range in $\cos\theta$ is required. At fixed target machines it is possible to achieve a range of $-0.6 < \cos\theta < 0.6$ at $X_F = 0$. This will be adequate as the cross section will vary by approximately an order of magnitude over this range of $\cos\theta$.

Intensity

The cross section for di-pions as measured at the ISR was parametrized as

$$\int_{-0.4}^{+0.4} d\cos\theta \int_{0}^{1} dp_T \left. \frac{d\sigma}{dm\, dY\, d\cos\theta\, dP_T} \right|_{Y=0} = \frac{1.0 \times 10^{-27}\, e^{-14.1\, m/\sqrt{s}}}{m^{6.5}}$$

Therefore to reach both high mass and high X ($\equiv m/\sqrt{s}$) the highest energies and highest intensitites are required. The proposed experiment depends on accumulating integrated luminosities of approximately 10^{39} cm^{-2} for <u>both</u> the π^- and proton exposures. The measurement must also reach a transverse momentum scale where the power law dependence of the one particle inclusive cross section is observed[1] to

approach point like behavior ($p_T^{-5.5}$ at p_T > 10 GeV/c). In this realm the comparison of the single particle and di-hadron cross sections is informative by providing a stringent test for theoretical calculations. For this reason, running at the Tevatron is essential. At 400 GeV this region of transverse momentum is unattainable.

The proposed wide band Proton East beam will produce π^- intensity of 3.0 x 10^8/sec at 650 GeV/c for a proton intensity of 2.5 x 10^{11}/sec at 1000 GeV. Given a 20 second spill, a 10% interaction length hydrogen target, and an 800 hour run the integrated luminosity is $\sim$1.2 x 10^{39} cm^{-2}. The detector would run at 3 x 10^7 interactions/sec in this mode. It is designed to be able to run at rates as high as 10^8 interactions/sec with a dead time of less than 10%.

Suitability of other detectors

Detectors exist at Fermilab which might be considered as candidates for such a measurement. All appear to have serious limitations in either acceptance, rate capability, or magnetic tracking resolution. Both the focussing spectrometers (E605, E615) have only opposite sign pair acceptance. E615 has large $\cos\theta$ acceptance but only for low masses (~ 5 GeV/c), and mainly at large X_F. E605 has good high mass acceptance but only for values of $|\cos\theta| < 0.25$ (and only by allowing a variation in the acceptance of an order of magnitude). Over this range the deviation from a flat distribution is approximately 40%. The two calorimeter experiments (E609 and E557) are both inadequate in momentum resolution and rate capability. In addition, the M6 beam line cannot deliver the intensity which is required.

The Detector

The proposed experiment is to be conducted with a high resolution charged particle spectrometer which is to be triggered calorimetrically. The overall layout of the apparatus is shown (as planned for the highest energy running) in figure 3. The upstream tracking is done with three stations of proportional wire chambers equipped with "mini drift" readout. They are positioned at distances of

1.5m, 2.5m, 3.0m from the target, and have wire spacings of 1mm, 1.5mm, and 2mm respectively.

The analyzing magnet is centered 4m from the target, and has a horizontal field (x). The downstream tracking is performed with 3 stations of proportional wire chambers with mini drift each separated by 1.5m, the last one being 9.5m from the target. These have wire separations of 2, 2.5 and 3mm. The 3 upstream stations each have 4 views (x,y,u,v) to enable high multiplicity pattern recognition and provide sufficient vertex resolution in the bend plane. The downstream stations have 3 views (u,v,x) with the small angle stereo views providing the momentum measurement. There are a total of ~ 3700 wires in the front three stations and ~ 6000 wires in the back three. A scintillator hodoscope is placed between stations 4 and 5 for timing information and triggering.

On reviewing the proposed beam lines for the Tevatron the most reasonable beam line for this experiment appears to be the new P East beam needed by Experiment #687. It will deliver a very high intensity of π^- at very high energies. A further advantage is that with a few minor modifications the second analyzing magnet in that experiment would serve perfectly in the experiment being proposed. With this double use in mind the magnet could be mounted on rails and

the experiments designed to facilitate its movement. In order to match the acceptance for the lower energy (~400 GeV) running with the high energy (650 GeV) running the width of the magnet should be increased to ~1.2m from its present dimension of ~1m. As the beam energies are changed the length of the spectrometer is varied to optimize acceptance and tracking resolution.

As symmetrically triggered high P_T events have a large wide angle multiplicity (~10), we believe the vertex can be reconstructed in the xy plane to σ~300μm in a 10% interaction length hydrogen target (and 150μm/station or ~200μm/plane resolution). The resolution in z is ~2mm. With the vertex used in the momentum fit the momentum resolution (again assuming σ_x=200μm/plane) is calculated to be ~2% at 200 GeV/c.

To survive the high interaction rate desired, the detector must be insensitive to the majority of beam jet particles. The downstream chambers are completely deadened in the central area corresponding to ~θ<20 mr in the 650 GeV/c configuration. The upstream chambers are deadened over a larger region (θ < 40 mr). This is to ensure that the vertex detection does not define the maximum beam intensity. For symmetric high p_T pairs the wide angle multiplicity observed at the ISR was approximately 10

particles/interaction.[6] Therefore these chambers will typically reconstruct the vertex with approximately 7 particles. Furthermore, one of the pair will always be observed in the upstream chambers to ensure the correct vertex can be identified.

To protect the downstream chambers from low angle particles, which would be deflected by the magnet into their active region, a superconducting magnetic shield is inserted in the magnet. The shield is aimed at the target, shielding the field in the region $\theta<20$ mr. It will be a thin super conducting pipe cooled from the inside by helium gas during operation. The pipe is in a vacuum vessel which fills the magnet, thus the only material in the high particle flux region (small θ) is the NbSn and the super insulation around it. The gas pressure easily compensates the magnetic pressure.

Trigger

The function of the calorimeter is to trigger the apparatus on high P_T interactions and particularly those with 2 opposite high P_T particles. It is important to realize that the calorimeter is only used for the trigger. The analysis is performed completely with tracking in order to minimize the systematic errors from calibration. The

only requirement on the calorimeter is that the trigger can be made tight enough that the events for which the trigger is fully efficient represent a reasonable fraction of all triggers taken. This in turn implies a segmentation on the order of the hadronic shower width, for single particle identification. The calorimeter will also have a 20 mr hole.

To satisfy the segmentation requirement the calorimeter will have a fly's eye structure with wave shifter readout. We would propose to duplicate the MPS calorimeter design but with 6 inch cells. Acrylic scintillator will be used, which will be cut by laser so no polishing will be required. There will be electromagnetic and hadronic sections requiring a total of 600 phototubes.

Calibration

The most critical source of systematic error arises from small energy calibration errors that vary with $\cos\theta$. If the mass scale varies by only 3% as $\cos\theta$ is varied over the acceptance of the apparatus, the angular distribution will be distorted by 20% due to the steep mass dependence of the cross section. This type of error dominated the ISR measurement. By doing the measurement with tracking, and

calibrating the detector on known resonances, this error can be minimized. Given the extremely large integrated luminosity the dimuon resonances (ψ and T) are well suited for this purpose. By studying the mass of these resonances as a function of $\cos\theta$, the major systematic error will become negligible. Furthermore, the continuum has a characteristic shape $(1 + \cos^2\theta)$ which will allow a cross check on the acceptance calculation. The large π^- exposure ($\int Ldt \sim 10^{39}$) and large acceptance allow a dimuon continuum measurement of very high quality for the highest energies where all experiments are proton limited.

Muon Detection

Behind the calorimeter a muon detection system is planned for the detector calibration on dimuon resonances (ψ,T) and continuum. The design is chosen with careful consideration to the trigger backgrounds for dimuons (mainly halo and low momentum π decay). The calorimeter is followed by a passive steel filter to stop any leakage from the calorimeter. A hodoscope in the non bend view is followed by more steel and a second hodoscope. These hodoscopes form roads which point to the target. This enables the use of a simple, fast analog circuit for finding hits in the non bend chambers consistent with a track originating from the target. The second muon hodoscope is followed by magnetized

steel with the field aligned to bend the previously unbent momentum component. The subsequent hodoscope allows a momentum cut on each muon. This system will allow an effective mass cut to be made in a time of ~300 ns. The muon detector also has a 20 mr hole in it with the beam dump placed behind. The total length of the detector from target to dump is ~15m.

Electronics and data acquisition

The electronics required for this detector consists mainly of ~10K channels of TDC's and ~1200 channels of ADC's for the calorimeter.

The TDC's are almost identical to those designed by W. Sippach for the Lab E upgrade (E-652). The events are buffered in a memory on each card which provides a large data compression. The cost of all the electronics for the wire chambers would be ~ $300K. This includes power supplies, racks, crates, cables, amplifiers, discriminators, etc.

The ADC's must cover a large dynamic range and have a fast conversion time. We propose using two 10 bit ADC's for each phototube. The LeCroy ADC designed for E-605 has a 4 μsec conversion time for a cost of $30/channel and

satisfies the requirement. Each ADC module will have a buffer memory associated with it. The buffer memories could be filled in parallel so that the dead time from the ADCs would be less than 30 μsec. This system will allow ~300 events/spill to be taken with less than 10% dead time. The multi event buffers for the TDC's and ADC's will be read into the computer between spills.

Acceptance

To measure the angular dependence of the quark-quark interaction by this method, the largest acceptance in polar angle ($\cos\theta$) possible at $X_F \sim 0$ is necessary. Again stressing the measurement is best performed at low X_F so that at finite and attainable values of $m/\sqrt{s}$ both beam and target quarks will be in the valence region, $x > 0.3$. The acceptance of the detector is shown in figure 4 in terms of $\cos\theta$ vs X_F for massive states (at $p_T=0$) where the spatial deflection of the magnet is not an issue (m=10 GeV). The acceptance is 100% for most of the region $|X_F| < 0.2$, $|\cos\theta| < 0.6$. With this uniformity in acceptance it will be possible to observe the small (~10→20%) expected differences in the shapes of the same and opposite sign pairs. To illustrate the importance of this, the shapes of the expected and observed angular distributions (without acceptance corrections) are shown for the proposed

experiment and the focussing spectrometer E605 in figure 5.

Interaction Rate

A simple Monte Carlo simulation was performed to calculate the maximum intensity at which the experiment could run. The central region "minimum bias" particles were generated with a distribution of

$$\frac{dN}{dP_T dy} = 18\ p_T e^{-5p_T^2}$$

which corresponds to 1.8 charged particles per unit rapidity and the observed low p_T distribution.[7] This calculation indicates that the rate is limited by the central wires in the non bend view of the chamber just downstream of the magnet. The double peaked structure seen in figure 6 is due to the circularly deadened region in the center ($\theta<20$ mr). These wires run at twice the rate of any others maximum rate of ($1 \times 10^5/10^7$ interactions/sec). By adjusting the shape of the deadened region in this view and/or by decreasing the wire separation in bands around these peaks we expect to run a a rate of 10^8 interactions/sec with these wires running at less than 600 kHz.

One Particle Inclusive Data

There are two main sets of data of inclusive high P_T hadron production:

a) The Chicago-Princeton group (E-300, E-258)[8,9] on charged hadron production (π^+, π^-, K^+, K^-, p, $\bar{p}$) with proton and π^- beams

b) The ISR data of the CCOR,[1,6] Athens-Yale,[10] and CSZ[11] groups on π^o production where the π^o was detected through its decay into two photons.

The Chicago-Princeton data extend to a P_T of ~7 GeV/c with the proton beam and to ~6 GeV/c with the π^- beam. From dimensional arguments the invariant inclusive cross sections of high P_T processes should be parametrized as:

$$(1) \quad E\frac{d^3\sigma}{dp^3} \alpha \frac{1}{P_T^n} (1-X_T)^m \qquad X_T = \frac{2P_T}{\sqrt{s}}$$

The exponent n should equal 4 if the basic interaction is quark-quark scattering through a gluon exchange i.e first order QCD diagram. The Chicago-Princeton data can be fit to the form of Equation (1). However n comes out to be ~8 for

mesons and ~11 for p's and $\bar{p}$'s.

The ISR data on π^o production extend to P_T values of ~15 GeV/c. The data of references 1,6,and 11 show a clear decrease of the power n to a value of 5.5 at P_T>10 GeV/c. However the data of reference 10 do not show an indication of decreasing n. There are experimental difficulties with the ISR data, among them, the contribution to the π^o signal from single high P_T photons.

The model of reference 12 explains the fact that n=8 rather than 4 in the 2→7 GeV/c P_T region as being due to a series of effects:

a) The distribution and fragmentation functions of quarks and gluons are not only functions of X but also of Q^2 (scaling violations).

b) The coupling constant varies with Q^2.

c) The intrinsic transverse momentum of the partons (Fermi motion).

The effect of parts a and b is to raise the power n by 2 units from 4 to 6. Part c raises the power by another two units achieving reasonable agreement with the data. The calculations[12] indicate that the power law should fall asymptotically to 4 as p_T is increased as was observed in the ISR data.[1,6,11]

It will be of great theoretical interest to see if n approaches 4 at higher p_T. In the proposed experiment we will be able to extend the single <u>charged</u> particle inclusive measurement to P_T values of ~14 GeV/c (for $\sqrt{s} \simeq 35$ GeV see Table I). This is a factor of ~2 higher than the existing data. This can be done by having a single particle high P_T trigger running in parallel with the di-hadron one. A potential difficulty associated with this measurement could be the lack of particle identification. However this is not a very serious problem since:

1) The p/π^+ and $\bar{p}/\pi^-$ ratios are already very small[8,9] at ~6 GeV/c (~10% and 1% respectively). Therefore the baryons can be neglected.

2) The K^+/π^+ and K^-/π^- ratios[8,9] are about 40% and 20% for $P_T > 2$ GeV/c and approximately constant (as a function of P_T) for both proton and pion beams.

Another important outcome of the proposed experiment will be the study of the angular dependence of the ratio

$$(2) \qquad \frac{\pi^- + N \rightarrow h^- + X}{\pi^- + N \rightarrow h^+ + X}$$

over larger ranges of P_T and θcm than the existing measurement. The one particle inclusive measurement serves as an overall check on the experiment by comparing the low p_T data ($p_T < 7$ GeV/c) with the existing measurements.[8,9]

Multi Particle Correlations

One of the properties that makes this experiment unique is its ability to accumulate a large integrated luminosity (in finite time) while detecting the majority of particles in the central region. While there have been many hadronic experiments which have attempted to observe jets, like those seen at PEP and PETRA, the fact remains that they have not been successful in the same way. A naive scan of events from hadronic experiments does not impress the viewer the way the e^+e^- events do. It is not difficult to understand this if the Fermi motion of the initial state quarks is considered. A 7 GeV/c P_T single particle would be associated with a recoiling jet of only 3-5 GeV/c p_T. This

corresponds to SPEAR energies where the jet structure could only be seen through a complex analysis. At 10 to 12 GeV/c P_T where this experiment is expected to have tens of thousands of events, the recoil jet would have 6 to 10 GeV/c P_T, much more like PEP/PETRA energies. Furthermore, given the large value of X_T (~ 0.5) in the π^- run, most of these jets will be well within the acceptance of the detector. At these transverse momenta the non observation of recoil jets (at the scanning level) would pose serious difficulties for the standard model of high transverse momentum production.

Summary

We propose an experiment that measures the energy, angular and flavor dependence of massive di-hadron production over a large angular range, interpreting the data as constituent scattering. This experiment will provide a fundamental data set to test QCD or other hadron interactions theories.

The detector is a calorimetrically triggered large aperture forward spectrometer with large acceptance, capable of operating at a high interaction rate. The detector would cost $900K if all new material were used (as little as $300K if major equipment were shared) and would be ready in about a year. We suggest using the new high intensity pion beam in P-East at 400 and 650 GeV/c. We request about 1700 hours of beam time.

Appendix A

Comprehensive data on the structure of proton-proton interactions in which a high transverse-momentum particle is produced was accumulated by the CCOR collaboration at the CERN ISR, and presented in the theses of D. Levinthal (Nevis Laboratories, Report 235, 1980) and J. Yelton (Oxford University, 1981). The CCOR apparatus determined the momenta of charged particles over the full azimuth, ϕ, and the rapidity range $-0.7 < Y < 0.7$. The analysis summarized here considers only events in which the triggering particle P_T was greater than 7 GeV/c.

Evidence for a jet-like structure recoiling against the trigger particle is given in terms of the variables P^{θ}_{out} and P^{ϕ}_{out} (see figure 7). The vectorial sum of the momenta of all charged particles produced in the region $|\phi^{particle} - \phi^{trigger} - 180^{o}| < 60^{o}$ defines an axis termed the "vector sum". The average multiplicity in the vector sum was 4.5. The momentum of each particle (in the sum) transverse to this axis is decomposed into two components, one in the plane of the beam and the "vector sum", P^{θ}_{out}, and the other perpendicular to this plane, P^{ϕ}_{out}.

The mean value of these components as a function of the transverse momentum is shown in figure 8. As can be seen, the values for $\langle P^{\theta}_{out} \rangle$ and $\langle P^{\phi}_{out} \rangle$ are essentially the same and constant (at ~ 350 MeV/c). This azimuthal symmetry around the vector-sum axis would <u>not</u> be expected if the particles included in the vector sum (i.e recoiling against the trigger) were mutually independent. Explicit calculation also shows that the azimuthal correlation between the trigger particle and the individual recoiling particles is not strong enough alone to generate a value of $\langle P^{\phi}_{out} \rangle$ as small as observed, giving values which are over 600 MeV/c and tend to rise with P_t. These two features of azimuthal symmetry around the vector sum axis, and strong correlations among the particles included in the vector sum are just the characteristics of a jet.

The enhancement in multiplicity and transverse momentum on the <u>same</u> side as the trigger is another well known effect, suggesting that the trigger particle is part of another jet. By summing the momenta of all the charged particles within an azimuthal angle of $\pm 60^{o}$ around the trigger, and correcting for neutrals, the fraction of the jet momentum taken by the trigger particle is obtained. As shown in figure 9, this fraction (Z_{trig}) is between 75% and 90%, rising with X_T.

REFERENCES

1. A. L. S. Angelis et al., Physics Scripta 19, 116 (1979).

2. This effect was given the name "trigger bias" by M. Jacob and P. Landshoff, Physics Reports 48C, 286 (1978).

3. R. D. Field, Phys. Rev. Lett. 40, 997 (1978).

4. R. Baier et al., Z. Phys. C. 2, 265 (1979).

5. Fermilab-Pub-80/96-EXP. 7420.180 to be published in Nucl. Phys. B.

6. D. A. Levinthal, Ph.D. thesis, Columbia University, 1980.

7. H. W. Atherton et al., CERN Internal Report 80-07 (1980).

8. D. Antreasyan et al., Phys. Rev. D19, 764 (1979).

9. J. M. Green, Ph.D. thesis, University of Chicago (1981) and N. D. Giokaris, Ph.D. thesis, University of Chicago (1981).

10. C. Kourkoumelis et al., Z. Phys. C. Vol 5, No. 2, p. 95 (1981).

11. G. Clark et al., Phys. Lett. 74B, 267 (1978).

12. R. P. Feynman, R. D. Field, and G. C. Fox, Phys. Rev. D18, 3320 (1978).

13. G. Wolf, DESY Report 81-086, (1981), courtesy T. Yamanouchi, private library.

FIGURE CAPTIONS

Fig. 1. Constituent scattering interpretation of high p_T production.[12]

Fig. 2. Angle dependence for the process $e^+e^- \rightarrow u^+u^-$.[13]

Fig. 3. The detector.

Fig. 4. Detector acceptance as a function of X_F and $\cos\theta$.

Fig. 5. Cross section times acceptance $v_s \cos\theta$.

Fig. 6. PWC profile first chamber downstream of magnet non bend view.

Fig. 7. Definition of variables in Fig. 8.

Fig. 8. Transverse momentum of fragmentation as a function of transverse momentum wrt beams.

Fig. 9. Fraction of trigger jet momentum taken by trigger particle v_s $X_T = 2\ p_T/\sqrt{s}$.

Fig. 10. Angular distributions from ISR data $\sqrt{s} = 45$.

Fig. 11. Angular distributions from ISR data $\sqrt{s} = 62.4$.

Fig. 12. Mass dependence of di-hadron production at the ISR. Also shown is first order QCD predictions.

Table I.

One particle inclusive event rates for π^- running based on E-258 data using fit.

$$\frac{A}{P_T^{\,n}} \quad (1-X_T)^b$$

A	n	b	
0.44×10^{-26}	8.6	7.0	π^+
0.32×10^{-26}	7.5	8.9	π^-

assuming $\int Ldt = 10^{39}$ cm^{-2} at 650 GeV/c π^-

P_T	π^+	π^-
5	1.27×10^7	2.85×10^7
6	1.73×10^6	4.14×10^6
7	2.89×10^5	6.72×10^5
8	5.18×10^4	1.11×10^5
9	9.7×10^3	2.0×10^4
10	1.8×10^3	3.2×10^3
11	3.2×10^2	4.9×10^2
12	50	57
13	7	6
14	1	1

If the ISR data prove correct and the power law approaches $P_T^{-5.5}$ there will be enormously more events at the highest transverse momenta listed. These are therefore to be considered conservative lower limits.

Table II.

Symmetric dihadron rates

m	$\sqrt{s}$ = 35	$\sqrt{s}$ = 41
8	1.9×10^5	3.1×10^5
10	2.0×10^4	3.7×10^4
12	2.8×10^3	5.6×10^3
14	454	1000
16	85	220
18	18	51
20		13

These rates assume an extrapolation of the ISR data over the larger angular acceptance and use the X dependence observed for pp collisions for both the proton and π^- runs. The assumed luminosity is $\int Ldt = 10^{39}$ and the cross section

$$\int_{-0.6}^{+0.6} d\cos\theta \int_{0}^{1} dp_T \left. \frac{d\sigma}{dm\, dY\, d\cos\theta\, dP_T} \right|_{Y=0} = \frac{3.6 \times 10^{-27}\, e^{-14.1\, m/\sqrt{s}}}{m^{6.5}}$$

The π^- estimates should be considered conservative because of the assumed X dependence. If the integration over P_T is performed over a larger range the number of events is greatly increased (times 4 for $\int_0^2 dp_T$).

Table III.

Costs

Chambers		
frames and construction		$ 100K
preamps/discriminator	~ $ 5/wire	
cable	~ $ 6/wire	
TDCs	~ $ 15/wire	300K
power supplies (chambers and readout)		12K
racks and crates		5K
Calorimeter		
steel		70K
lead		20K
scintillator		50K
phototubes	$100/tube	60K
ADCs	$ 30/channel	36K
Hodoscopes		80K
Iron magnet		100K
Superconducting pipe and vacuum box		100K
		$ 933K

This cost would be modified by using an existing calorimeter (E-687) with minor adjustments for the requirements of this experiment.

Table IV.

Running Request

beam	π^-	p
400 GeV/c	200 hrs at 10^9/sec $\int Ldt \sim 5 \times 10^{38}$	100 hrs at 10^9/sec $\int Ldt \sim 2.5 \times 10^{38}$
650 GeV/c	800 hrs at $3 \rightarrow 7 \times 10^8$/sec $\int Ldt \simeq 10^{39}$	
900 GeV/c		400 hrs at 10^9/sec $\int Ldt \sim 10^{39}$

In addition, 200 hrs are requested for an engineering run, to test the apparatus in place.

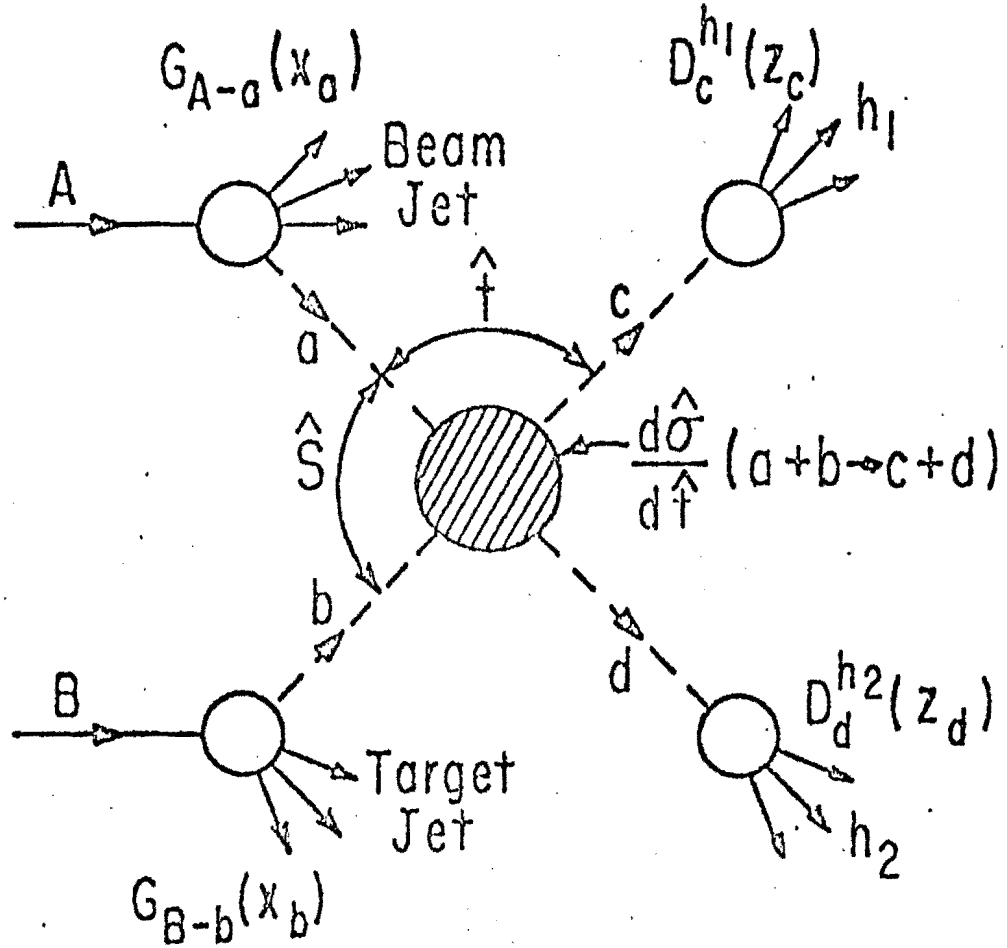

Fig. 1. Constituent scattering interpretation of high p_T production.[12]

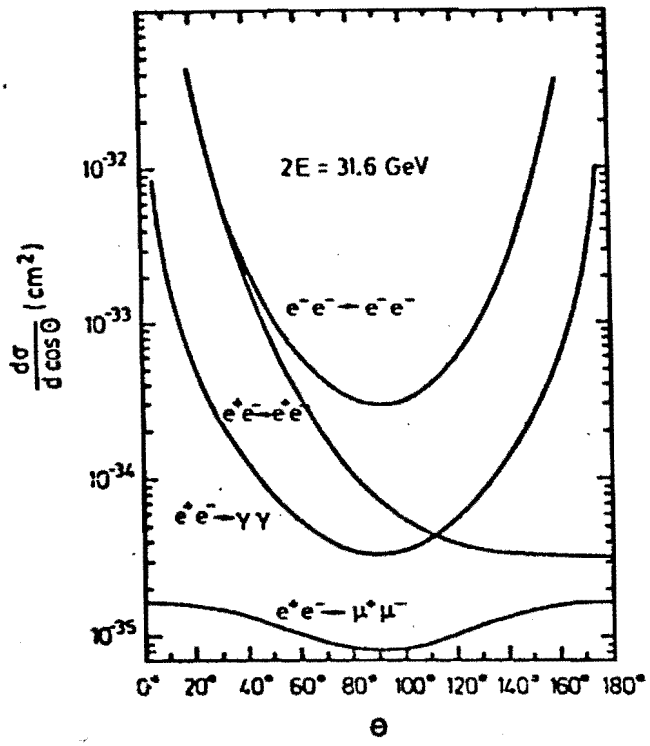

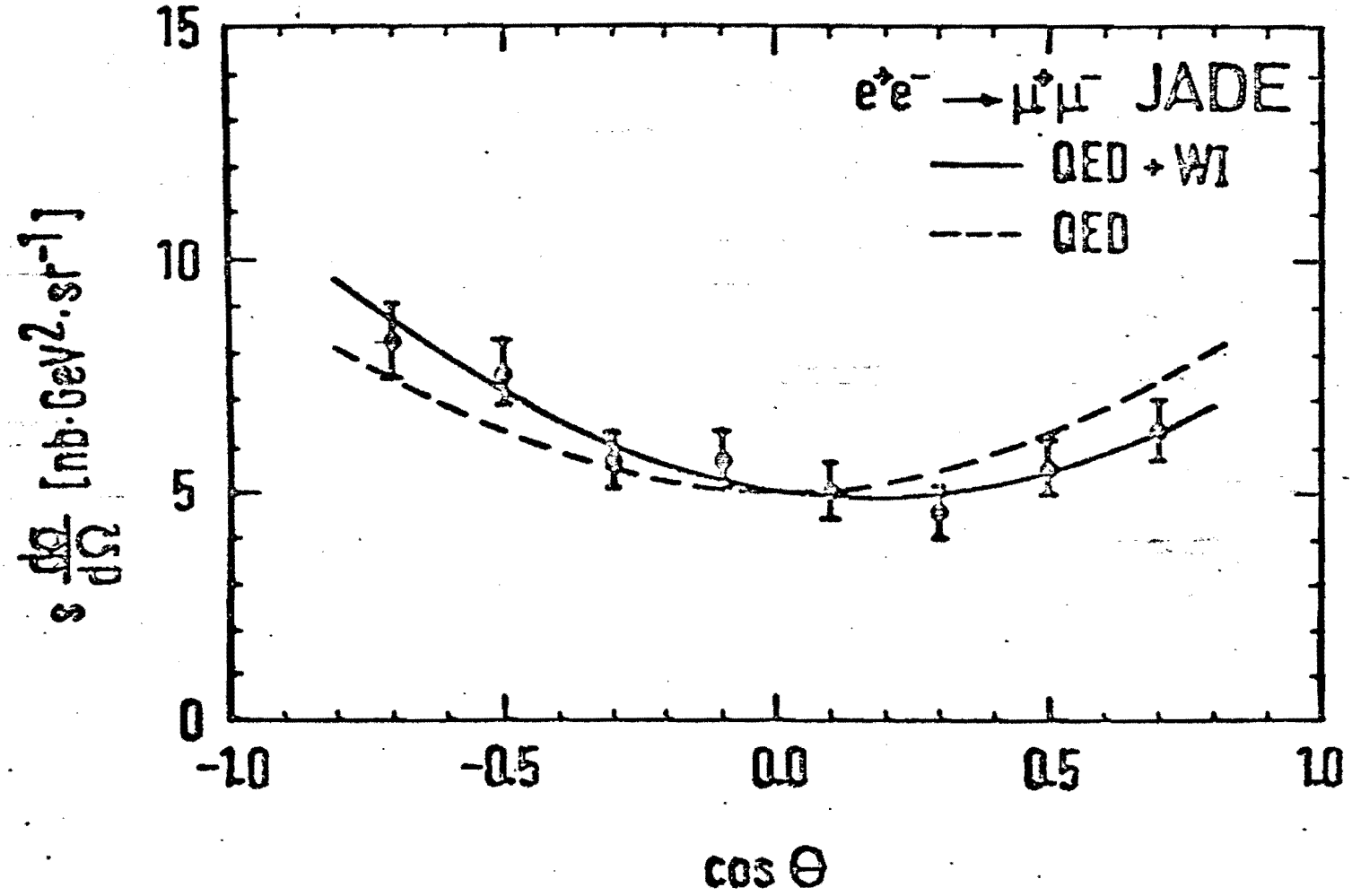

Fig. 2. Angle dependence for the process $e^+e^- \to u^+u^-$.[13]

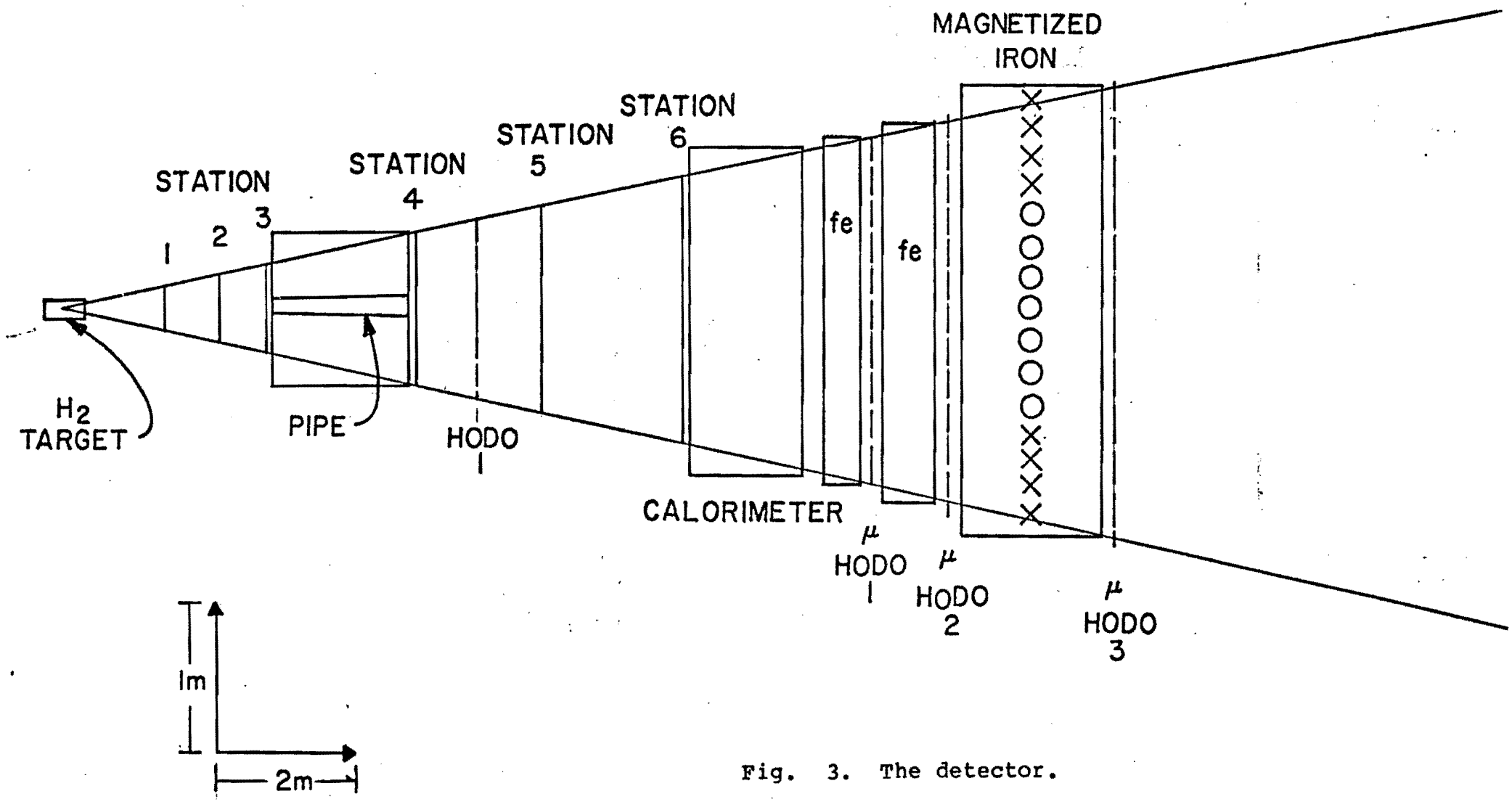

Fig. 3. The detector.

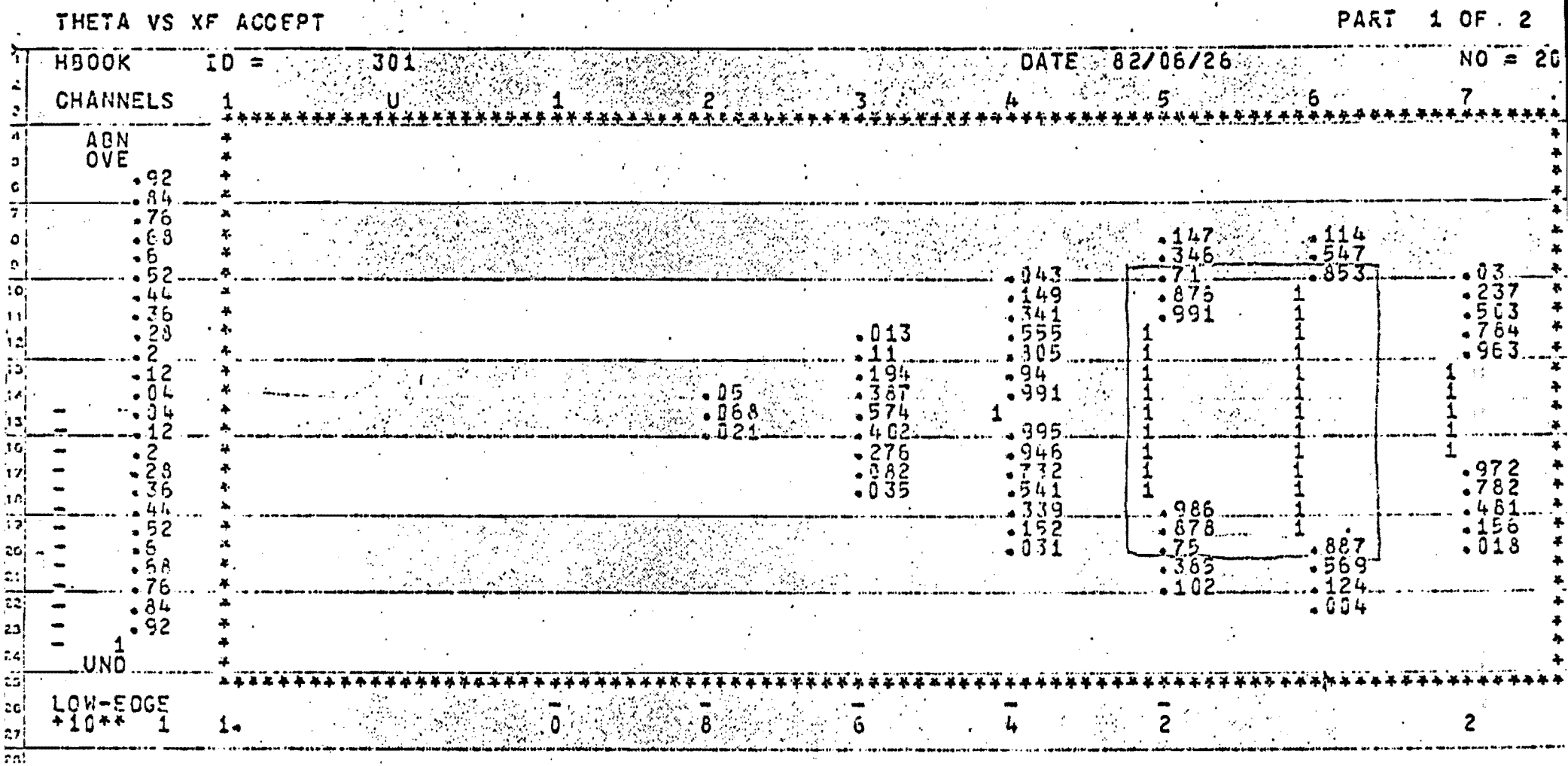

Fig. 4. Detector acceptance as a function of X_F and cosθ.

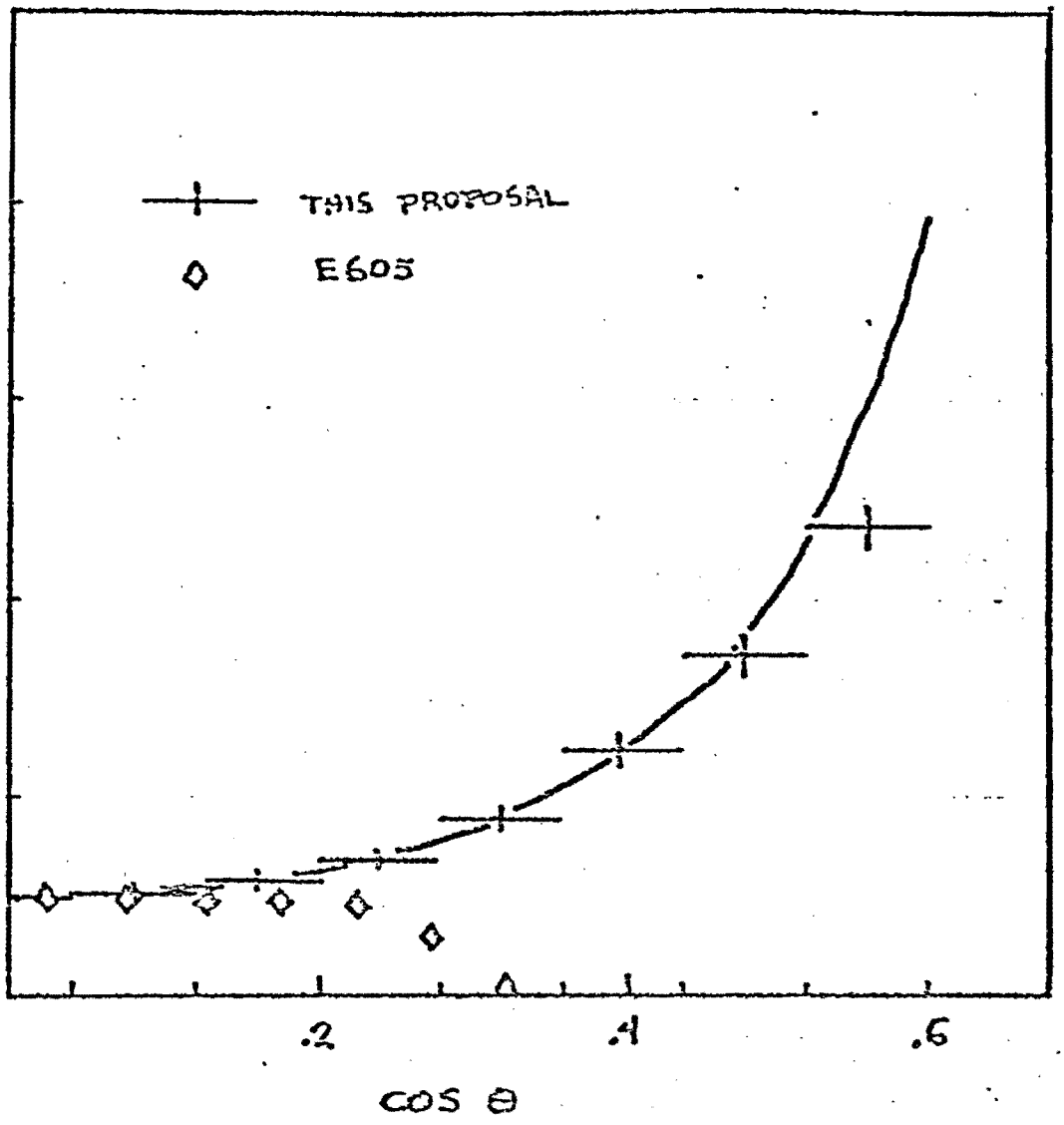

Fig. 5. Cross section times acceptance $v_s \cos\theta$.

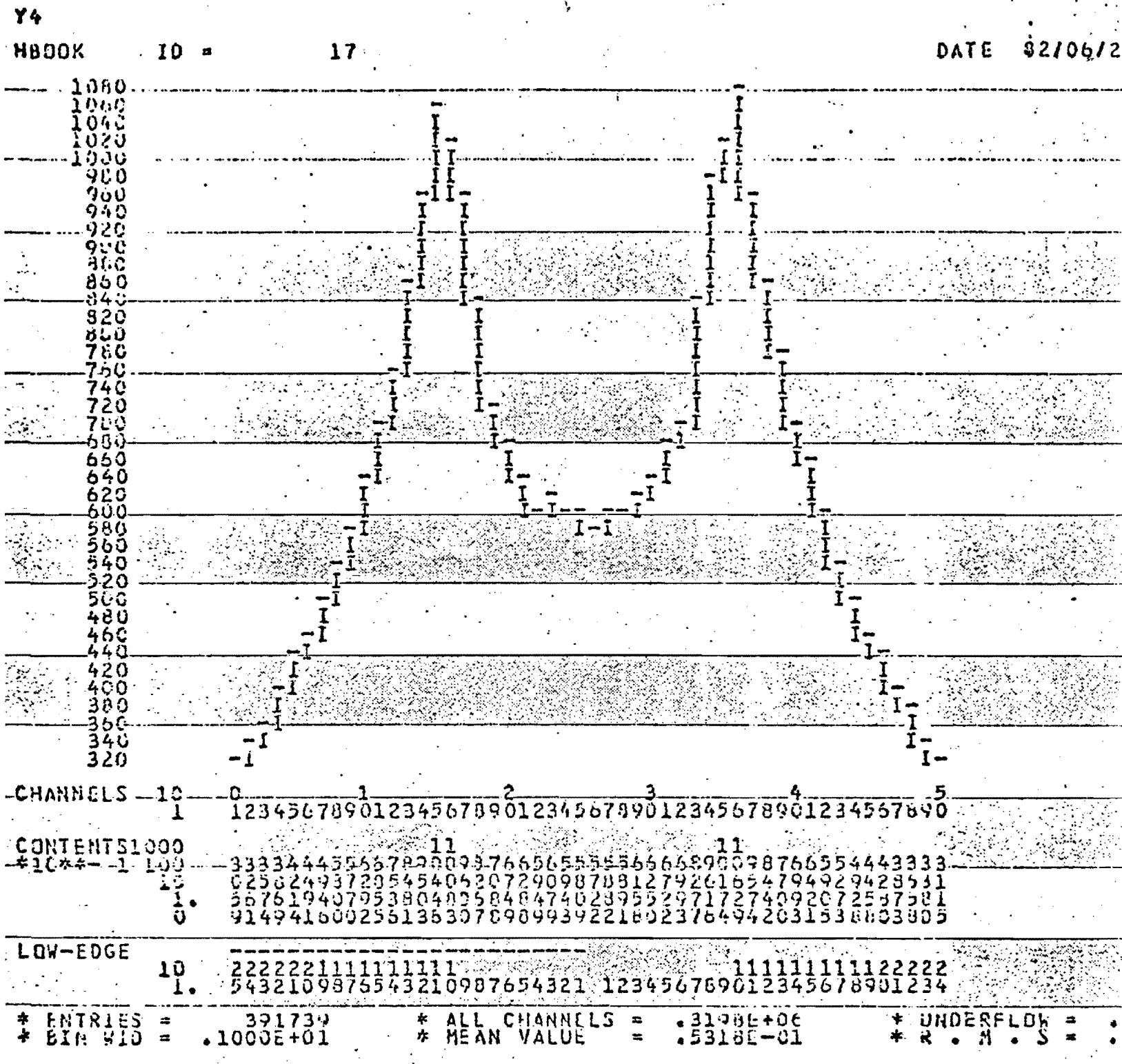

Fig. 6. PWC profile first chamber downstream of magnet non bend view.

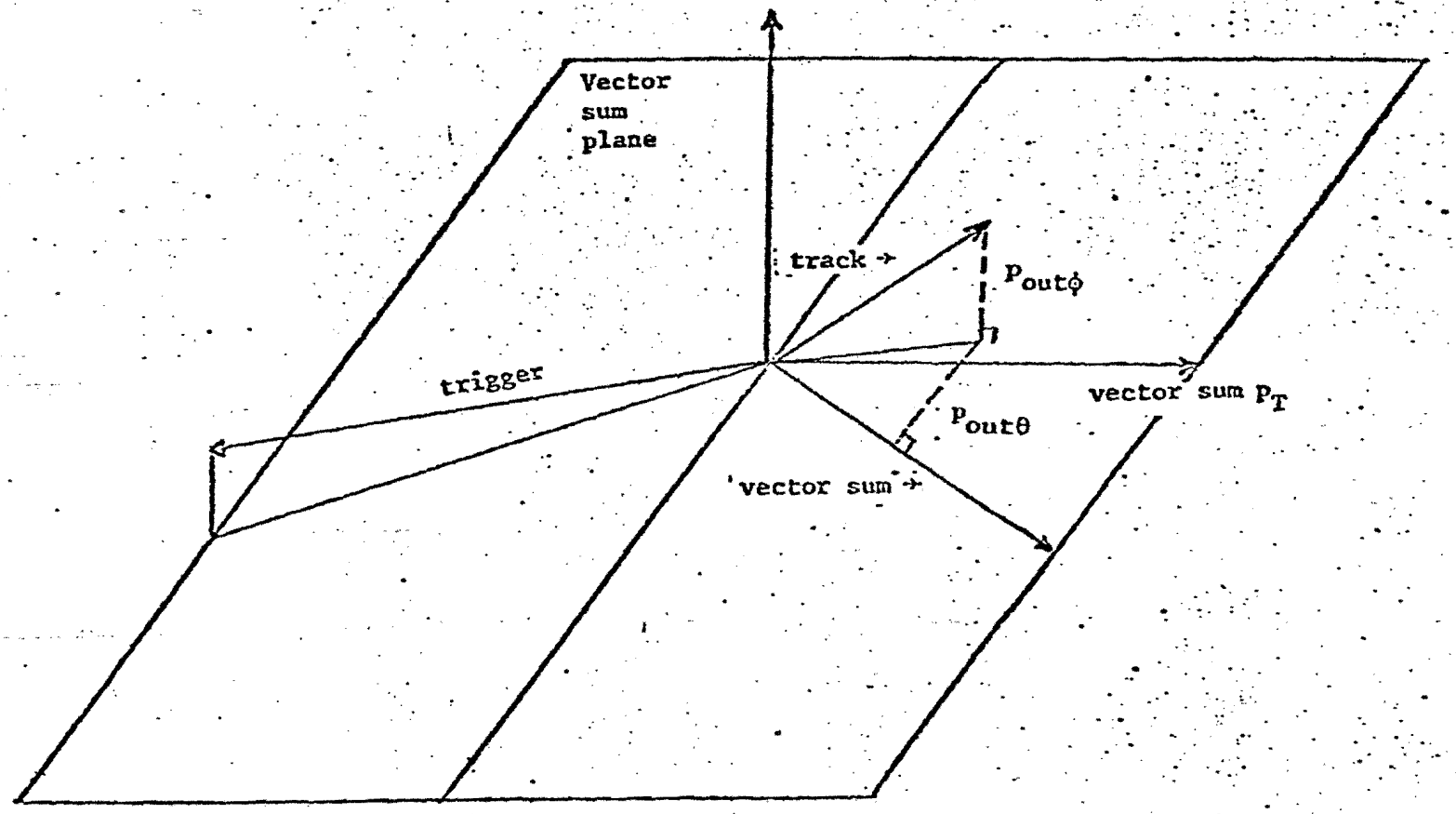

Fig. 7. Definition of variables in Fig. 8.

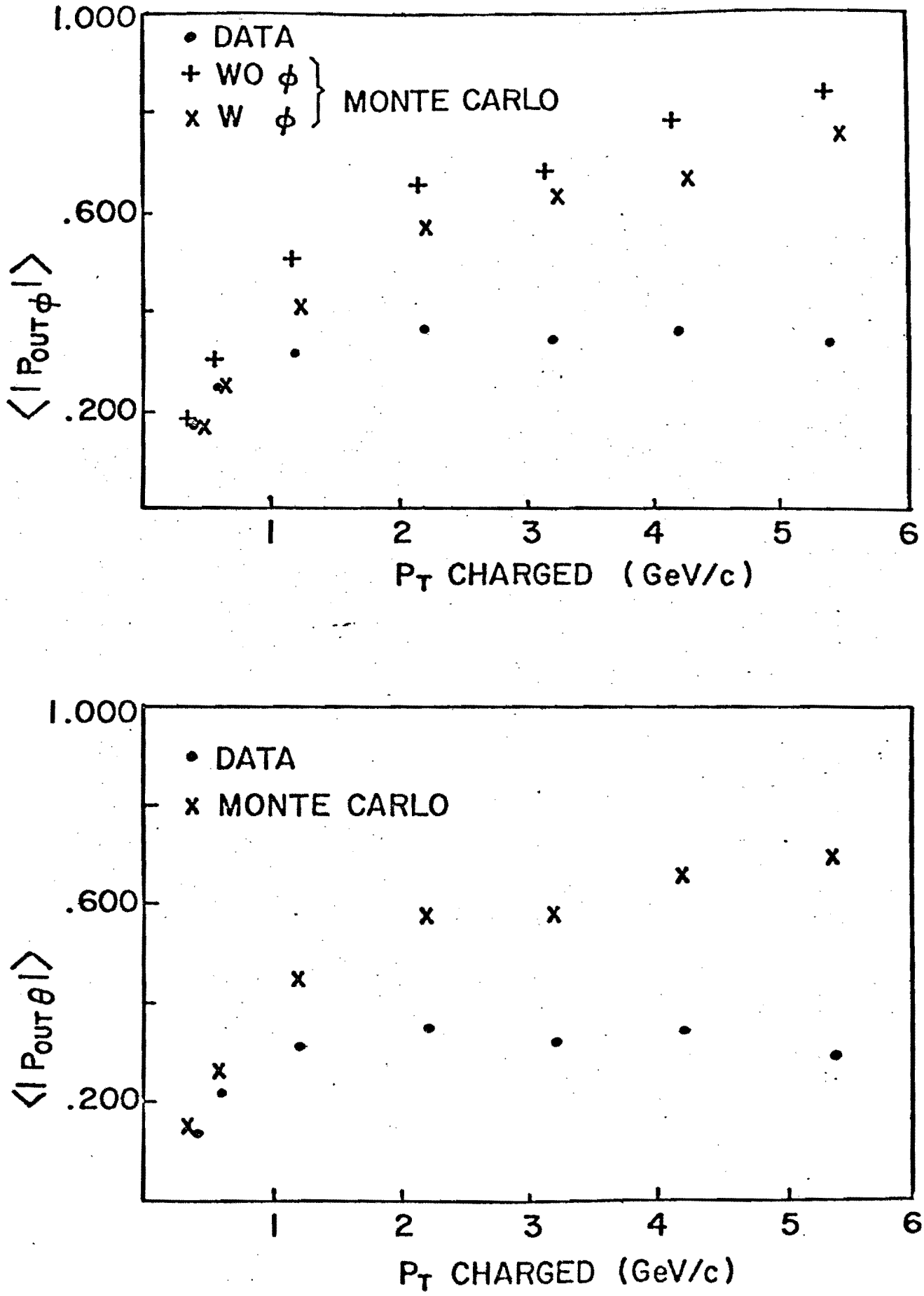

Fig. 8. Transverse momentum of fragmentation as a function of transverse momentum wrt beams.

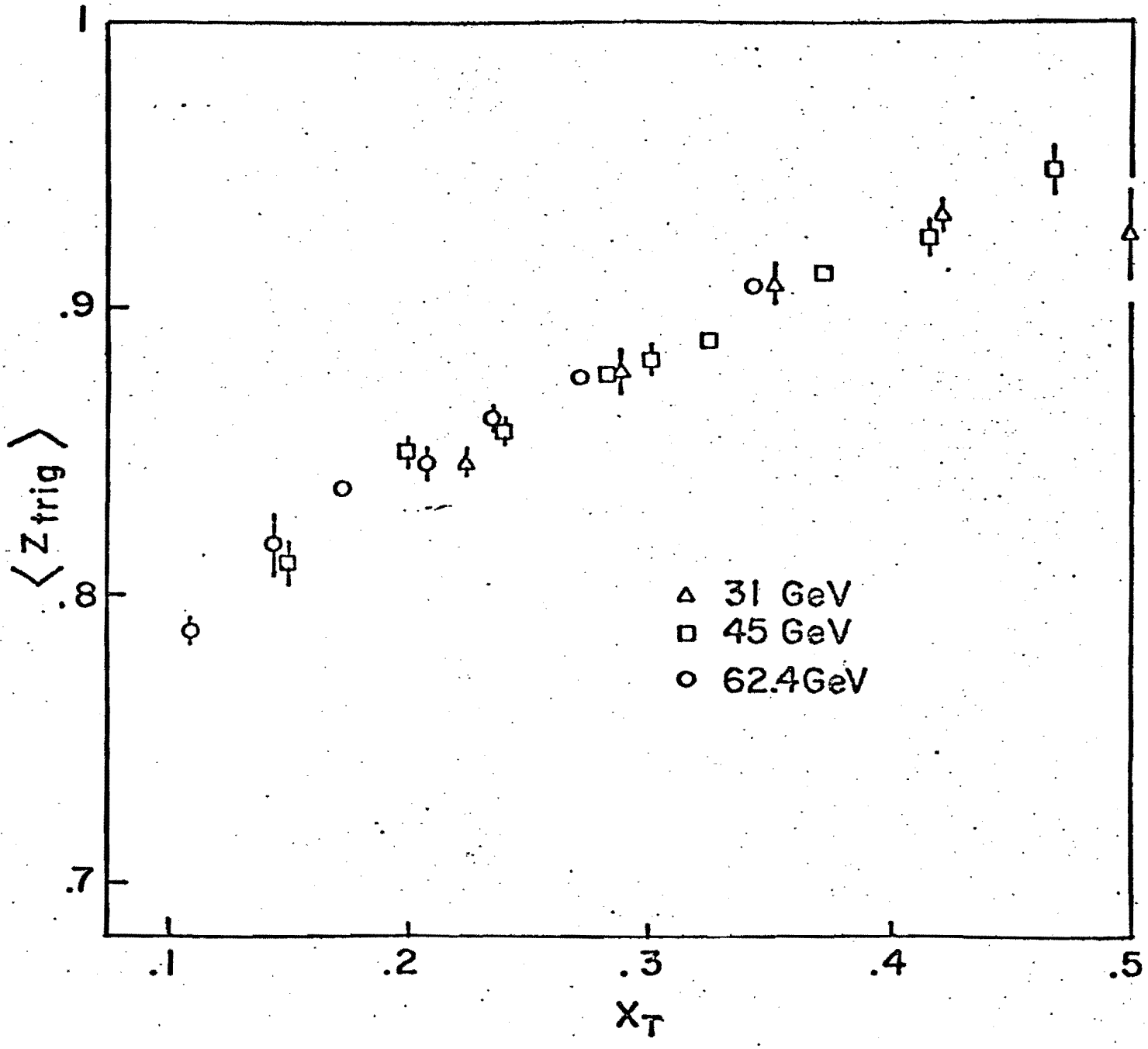

Fig. 9. Fraction of trigger jet momentum taken by trigger particle v_s $X_T = 2\ p_T/\sqrt{s}$.

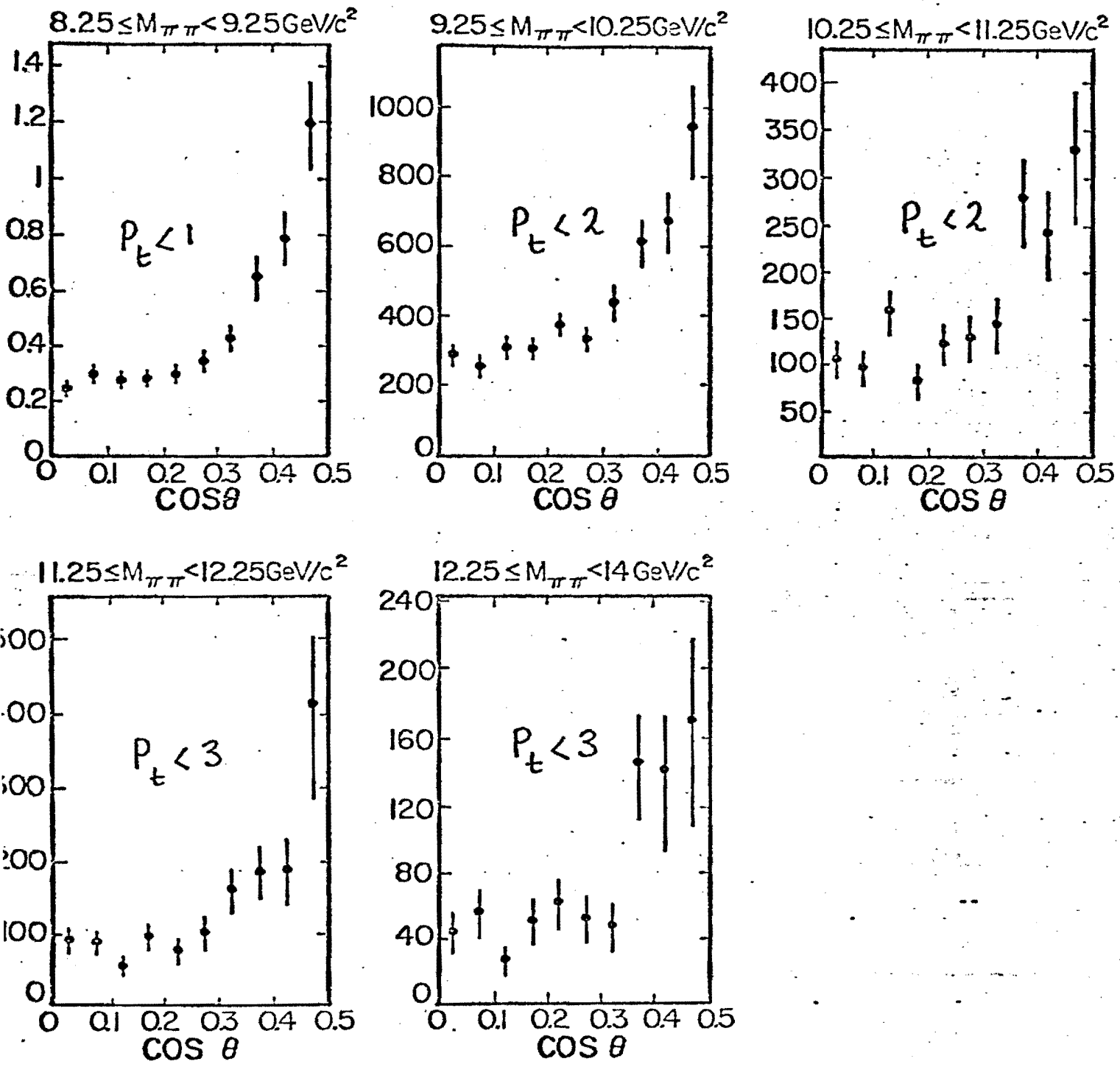

Fig. 10. Angular distributions from ISR data $\sqrt{s}$ = 45.

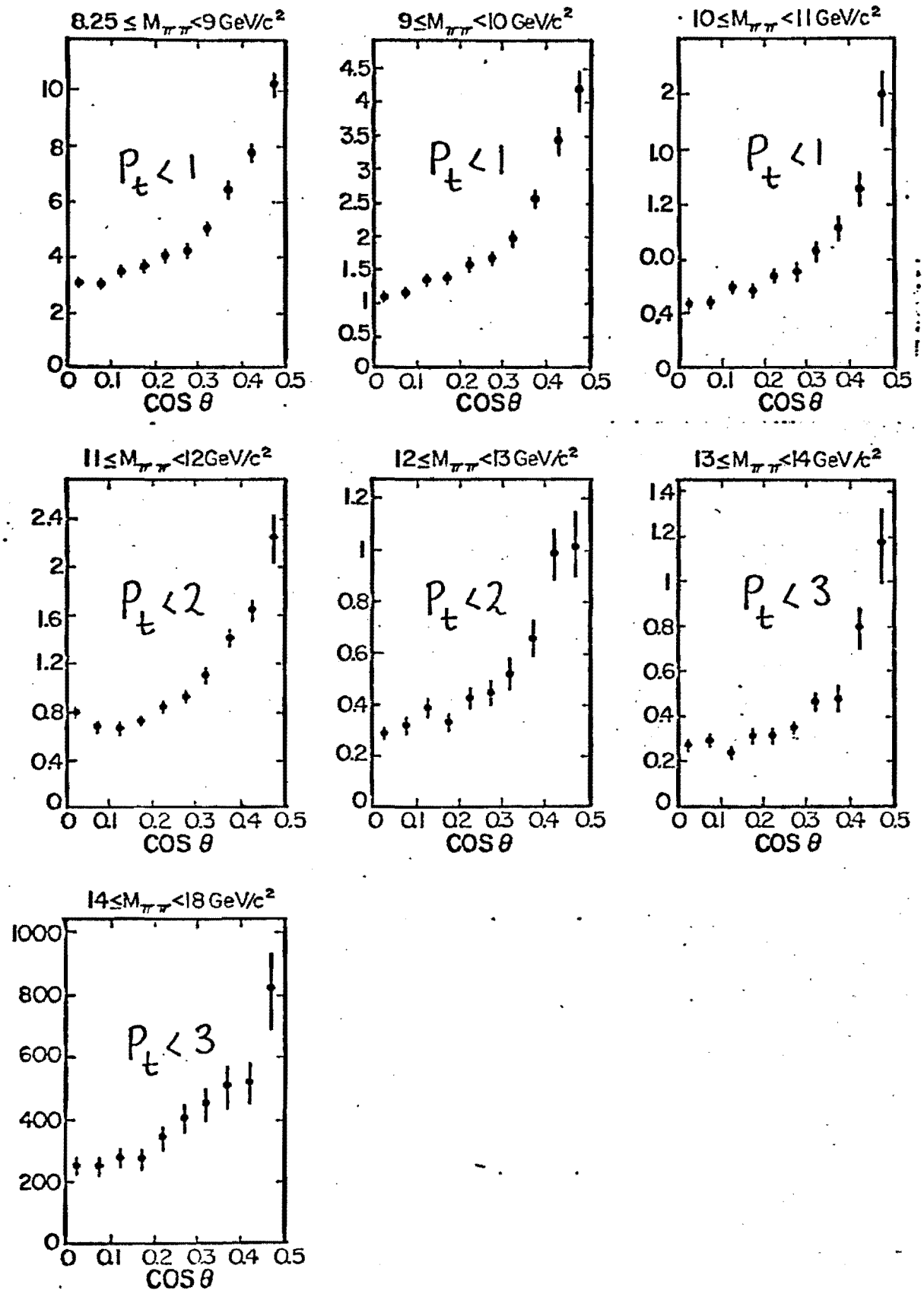

Fig. 11. Angular distributions from ISR data $\sqrt{s}$ = 62.4.

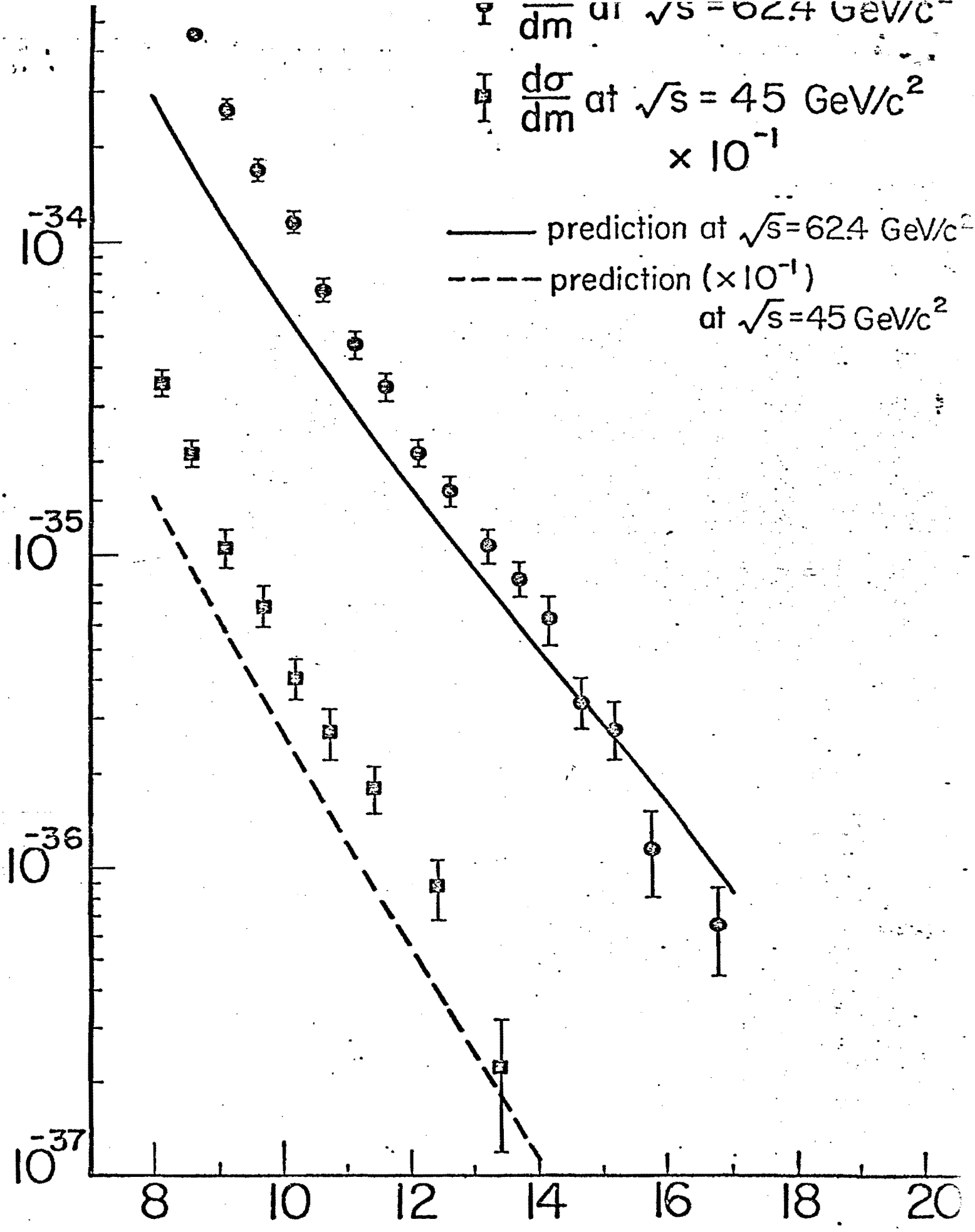

Fig. 12. Mass dependence of di-hadron production at the ISR. Also shown is first order QCD predictions.

04 April 83

A SIMPLE SPECTROMETER FOR STUDYING MASSIVE DI-HADRON PRODUCTION IN PROTON COLLISIONS

ADDENDUM TO P711

INTRODUCTION

The 711 proposal describes a detector designed with π^- running in mind (maximum acceptance, 10% target to take advantage of the limited available π^- beam intensity). Since no high intensity π^- beam will be available to us in the near future, we have investigated the possibility of a greatly simplified spectrometer which uses existing, available magnets and is optimized for a proton run which could take place as soon as January 1984 (in the MC beam).

THE DETECTOR

The measurement is to be performed with an open geometry magnetic spectrometer followed by a calorimeter which provides a trigger. The detector design is affected by two properties unique to proton beams:

1. The beam spot can be made sufficiently small that a narrow target can be used to determine the vertex.
2. Luminosity is not limited by the available proton beam intensity, so 2π azimuthal acceptance is not necessary.

We propose a spectrometer which consists of a point-like Be target followed by a momentum analysing magnetic field and tracking chambers. Vertex chambers are not needed since the target determines the vertex. We restrict the acceptance to ±22.5° about the vertical, and having selected a narrow vertical acceptance, orient the magnetic field to bend horizontally. This geometry has the following advantages:

1. The bulk of the particle flux is naturally deflected away from any detectors.
2. The transverse momentum is not distorted by the magnetic field.
3. The calorimeter is greatly simplified because it needs only vertical segmentation.

Figure 1 is a beam particles view of the acceptance of the detector. Figure 2 shows a plan view and elevation of the proposed detector. For the range $|\cos\theta|<.6$, $|Y|<.5$ the acceptance of this detector is constant at .8 for masses greater than 5GeV.

MAGNETS

The necessary momentum resolution and aperture can be obtained using a system of two magnets both of which are available during the next cycle. The first magnet is a

BM109 modified to run at 13Kg with a 20"gap. The modification consists of shimming the pole faces apart and adding an extra set of coils. Two such magnets exist at FERMILAB. The second magnet is a 100D40 currently located in the M3 beamline. This combination of magnets provides 1.5% momentum resolution at 100GeV.

TRACKING

The tracking system consists of four stations of mini-drift PWC s (constructed like PWC s but with time digitization to interpolate between wires). Each station has four views (x,y,u,v). Wire spacing is 2mm on the first two stations. The third and fourth stations have larger wire spacing (4 and 6mm) and field wires to improve drift time linearity. All chambers are desensitized in the central region where particle fluxes are large. The system consists of 4000 sense wires. Drift times will be digitized using the LeCroy 4271 TDC system.

THE CALORIMETER

The role of the calorimeter in this experiment is to provide a fast trigger for high P_T hadrons and hadron pairs. It must be able to operate in a high rate

environment and, to measure P_T, it must have fine segmentation in the vertical (θ) direction. We propose the simple construction illustrated in figure 3. The scintillators will be horizontal slats viewed by phototubes at each end. Several slats in z will be combined using lucite light pipes. The calorimeter will consist of an electromagnetic section (.25" Pb plates) followed by a hadron section (1" Fe plates). The maximum width of the segments is determined by trigger reqirements (smaller segments give a greater fraction of single particle triggers), while the minimum width is constrained by shower containment. A choice which satisfies both requirements is nine segments (three each of 4", 6", and 10"). With this choice each segment subtends roughly 10° in the center of mass. If we assume two electromagnetic sections and two hadronic sections the design requires 144 phototubes.

TRIGGERS

The experiment will trigger on high P_T hadrons and hadron pairs. The primary trigger is the symmetric hadron pair trigger which will require a high P_T particle in each calorimeter such that $P_T^1+P_T^2>M$, where M is the mass threshold. To form P_T for a calorimeter of N segments, we first form N-1 trigger segments each of which is the linear

sum of all tubes on two adjacent calorimeter segments (each tube is weighted by its θ so that this sum is P_T). The sum $P_T^1+P_T^2$ is then formed for each of the $(N-1)^2$ combinations of one trigger segment in each calorimeter A trigger occurs if any of these sums exceeds the mass threshold. A calculation by Fred Lopez (UIC) based on the Field and Fox jet Monte Carlo indicates that if calorimeter segments are chosen to subtend 10° in the P-P center of mass, then 10% of the triggers will contain a hadron pair that would have satisfied the threshold. A single particle trigger occurs if any trigger segment exceeds the P_T threshold.

BEAM

The MC beam has not been requested for the next cycle. It s current mode of operation is as a zero degree neutral beam. By making a small hole through the absorber, a proton beam can be made in the model of M6. To accomodate the experiment the beam must be pitched to a height of 6' at the target (2' above the nominal height). Preliminary calculations indicate that a beam spot of .75mm x 10mm can be attained in such a beam.

RUNNING REQUEST

To measure the di-hadron angular distribution in the desired kinematic range ($x>.35$) requires an integrated luminosity of 10^{39}. At an interaction rate of 5×10^{7}/sec a ten week run would give a luminosity of 1.2×10^{39}. A wire rate calculation based on bubble chamber data indicates that the chambers can operate at rates in excess of 2×10^{8}/sec.

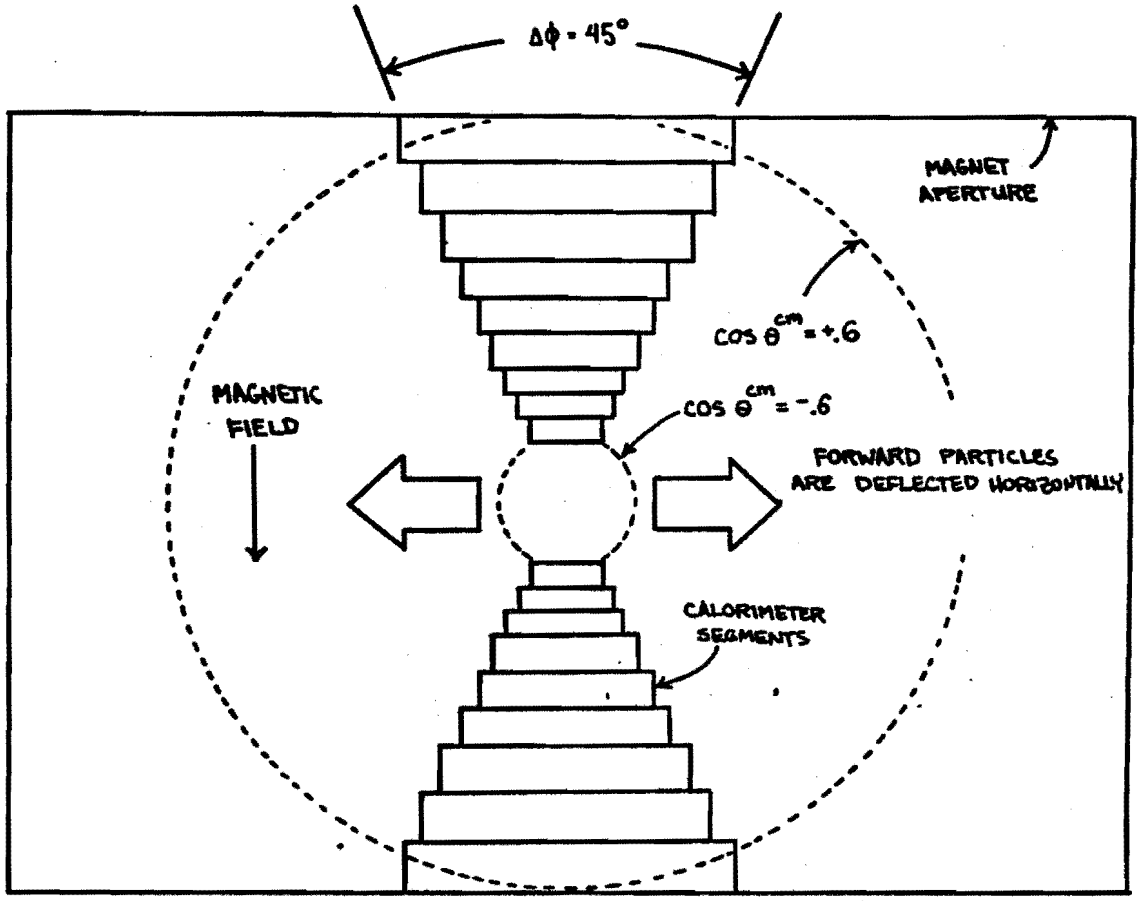

FIGURE 1: A beam particles view of the detector. Transverse momentum is measured in the vertical plane, magnetic deflection is in the horizontal.

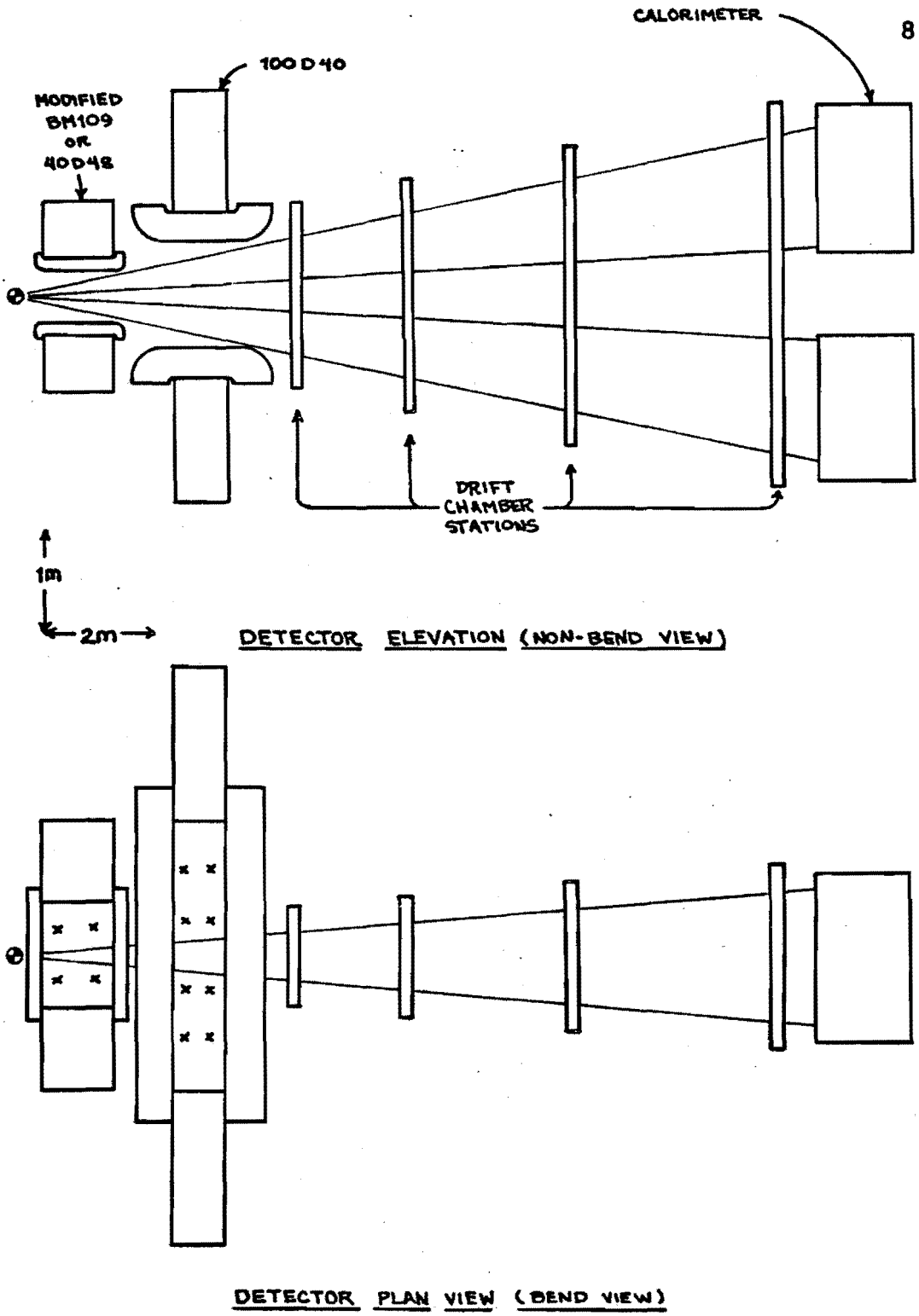

FIGURE 2: Plan view and elevation of the spectrometer.

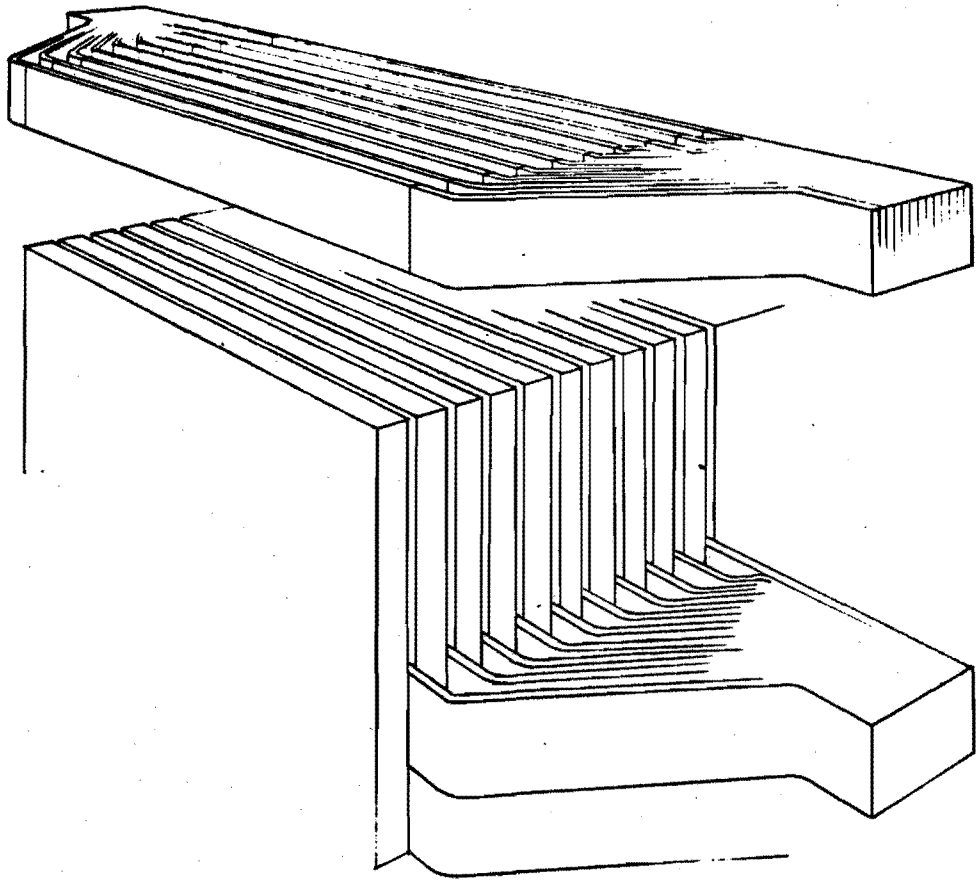

FIGURE 3: Calorimeter construction detail.